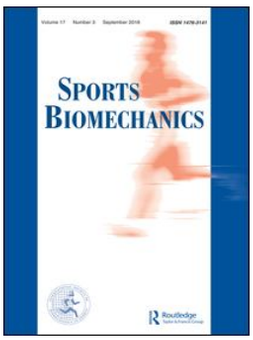

Sports Biomechanics

ISSN: 1476-3141 (Print) 1752-6116 (Online) Journal homepage: https://www.tandfonline.com/loi/rspb20

Cycling: joint kinematics and muscle activity during differing intensities

Wendy Holliday, Raymond Theo, Julia Fisher & Jeroen Swart

To cite this article: Wendy Holliday, Raymond Theo, Julia Fisher & Jeroen Swart (2019): Cycling: joint kinematics and muscle activity during differing intensities, Sports Biomechanics, DOI: 10.1080/14763141.2019.1640279

To link to this article: https://doi.org/10.1080/14763141.2019.1640279

Published online: 02 Sep 2019.

SPORTS BIOMECHANICS
https://doi.org/10.1080/14763141.2019.1640279

Routledge
Taylor & Francis Group

Cycling: joint kinematics and muscle activity during differing intensities

Wendy Holliday, Raymond Theo, Julia Fisher and Jeroen Swart

Division of Exercise Science and Sports Medicine, Department of Human Biology, Faculty of Health Sciences, University of Cape Town, Cape Town, South Africa

ABSTRACT

Full body kinematics and electromyographic (EMG) patterns may alter based on the workloads that are encountered during cycling. Understanding the effect of differing intensities on the cyclist can guide clinicians and bike fitters in improving specific muscle strength and cycling posture to optimise training and racing. We aimed to assess changes in lower limb EMG magnitudes and full body 3D kinematics of 17 well-trained cyclists at three different exercise intensities: 60%, 80% and 90% of maximum heart rate. Significant results were demonstrated for all the joints except the hip and shoulder. Cyclists' ankle dorsiflexion and knee extension increased between 6% and 9% with higher intensities. The elbow adopted a significantly more flexed position, increasing flexion by 39% from 60% to 90% intensity, whilst the lumbar and thoracic flexion increased by 7% at the higher intensity. There were significant increases in EMG signal amplitude at higher intensities for all muscle groups measured. These results will guide clinicians in strengthening specific muscles at specific ranges of the cycling pedal revolution. Guidelines for optimal bicycle configuration should take into account the full body position of the cyclist as well as the training and racing intensity when assessing kinematics.

ARTICLE HISTORY
Received 8 March 2019
Accepted 1 July 2019

KEYWORDS
Biomechanics; electromyography; bike fitting

Introduction

Optimal static bicycle configuration has been the topic of numerous studies (Bini, Hume, & Croft, 2011; Peveler, 2008; Peveler, Bishop, Smith, Richardson, & Whitehorn, 2005; Peveler, Pounders, & Bishop, 2007). The freely chosen bicycle configuration and subsequent cyclist kinematics, muscle activity and physiological responses can be influenced by adjusting any of the contact points on the bicycle (Burt, 2014). Previous research on the correct positioning of the handlebars, pedal crank arm length and saddle fore-aft position is based on personal perspectives and comfort (de Vey Mestdagh, 1998; Silberman, Webner, Collina, & Shiple, 2005; Burt, 2014), whereas static saddle height recommendations have been based on scientific methods. Currently, there are three main methods used in clinical practice to set the saddle height: anthropometrics (inseam length and trochanteric leg length), static knee

CONTACT Wendy Holliday HLLWEN005@myuct.ac.za

flexion angle methods and dynamic methods (during pedalling). The recommended static method is the Holmes method (Peveler et al., 2005). The cyclist is in a stationary seated position with the crank arm in the lowest or 6 o'clock position and the pedal surface in a horizontal orientation. Knee flexion angle (KFA) is measured with a goniometer and recommended to be in a range between 25° and 35° (where full knee extension is equal to 0°). It has been demonstrated that setting the saddle at this KFA range statically is optimal for injury prevention and performance (Peveler, 2008).

More recently it has been recommended that bike fitting be conducted in a dynamic functional manner, as kinematics can be influenced by cycling workload (Ferrer-Roca, Roig, Galilea, & Garcia-Lopez, 2012; Peveler, Shew, Johnson, & Palmer, 2012). With the advancement of technology, we are now able to record the cyclists' position in full three-dimensional motion capture, however as yet there are limited scientific recommendations for optimal joint ranges for dynamic bicycle configuration. Static recommendations for optimal bicycle configuration cannot be transferred to dynamic methods as the difference between static and dynamic lower limb angles has been highlighted (Bini et al., 2016; Fonda, Sarabon, & Li, 2014; Holliday, Fisher, Theo, & Swart, 2017; Peveler et al., 2012). The range of knee flexion recommended during static assessment using the Holmes method (25–35°) increases by ~ 5–8° (to approximately 30–40° KFA) depending on the study and the relative workload intensity (Farrell, Reisinger, & Tillman, 2003; Fonda et al., 2014; Peveler et al., 2012). Increased knee and hip extension were demonstrated at maximal workloads (Bini & Diefenthaeler, 2010; Bini, Diefenthaeler, & Mota, 2010) and could be linked to a shift in forward position on the bicycle (Bini, Senger, Lanferdini, & Lopes, 2012). This forward position on the bicycle was demonstrated during sustained high intensity cycling (Sayers & Tweddle, 2012). Increased sagittal plane thoracic angle (i.e., the thoracic segment moving anteriorly relative to the crank arm) occurred towards the end of the protocol and was suggested to be linked to cyclists shifting their body forwards as they fatigued, enabling more weight to be exerted onto the pedals. This was further confirmed where a greater trunk lean angle was demonstrated during a fatiguing protocol, with all participants also displaying an increase into dorsiflexion at the ankle joint (Dingwell, Joubert, Diefenthaeler, & Trinity, 2008). There was a positive association, such that an increase in EMG median frequency signal preceded an increase in movement kinematics. These suboptimal positional changes with fatigue may lead to maladaptive joint loading and thus may result in an increased risk of repetitive strain or long-term injuries. It was concluded that as fatigue occurs, cyclists changed their body position and muscle activation patterns to maintain performance (Dingwell et al., 2008).

The typical muscle activation pattern displayed during cycling has been studied in more depth due to the recent advances in technology (Hug & Dorel, 2009). Likewise, numerous studies have investigated muscle recruitment patterns in the final stages of exhaustion during cycling, and it is known that EMG patterns change with the onset of fatigue (So, Ng, & Ng, 2005). Lower limb muscle coordination during an all-out sprint cycling task displayed a significant change between the submaximal and maximal cycling exercises (Dorel, Guilhem, Couturier, & Hug, 2012). The increase in the duration of all muscle activity during the sprint is suggestive of a strategy to enhance the work generated by each of the muscle groups. During the all-out sprint, there was a large increase in hip flexor activity, a lesser extent to the knee flexor activity, whereas

the plantar flexors and knee extensors displayed an even smaller increase. It is possible that alternative muscles are recruited as fatigue accumulates in working muscles, as demonstrated by a decrease in Rectus Femoris EMG activity during all-out cycling sprints (Kay et al., 2001).

These studies were investigated at maximal power or to exhaustion and it is known that the body position on the bicycle and the muscle recruitment patterns are altered compared to riding at low intensities. Knowledge of how the muscles adapt to differing intensities, in conjunction with the position the cyclist is in, would help clinicians and bike fitters to strengthen those muscles in that range, at that cycling intensity. Racing at a workload of 55–60% VO_{2max} has been suggested as a strategic way to maximise power output while minimising the risk of early fatigue (Blake, Champoux, & Wakeling, 2012).

In order to maximise the use of muscle coordination patterns learned during training, it has been recommended that the cyclist train in similar conditions that they race in (Blake et al., 2012). The research published to date explores the adaptations of the lower limb kinematics and muscle activity with maximal effort or fatigue. The cyclist will, however, spend only a fraction of the race or training at absolute fatigue and/or maximal effort greater than 90% heart rate intensity, with the majority of the ride shifting between 60% and 80% heart rate intensity (Padilla et al., 2001; Palmer, Hawley, Dennis, & Noakes, 1994).

It is beneficial for clinicians and bike fitters to understand how the full body kinematics and lower limb muscles are affected by differing intensities encountered in cycling training and racing, not only with fatigue or maximal efforts. The only study to date that has assessed the relationship between workload intensity and 3D kinematics, demonstrated a small to moderate difference in lateral spine inclination and spine rotation between recreational and competitive cyclists (Bini et al., 2016). Currently, there are no studies investigating full body 3D kinematics simultaneously as well as lower limb muscle activity at differing intensities. The aim of this study was therefore to assess how the full body kinematics and specific muscle magnitude is affected by different intensities that are encountered in cycling. Furthermore, we aim to guide clinicians and bike fitters with recommendations for which joints or body segments to focus on during dynamic bike fitting and how cycling intensity during a bike fit may be of importance.

It was hypothesised that the upper body would adopt a more flexed position with intensity, whilst the ankle would move into a more dorsiflexed position and the knee into a more extended position, and that individual muscle activity would also increase proportionally. Furthermore, we hypothesise that the spinal segments and upper limb joints will demonstrate significant changes and that cycling intensity will have an impact on the bike fitting process.

Methods

Participants

Seventeen well-trained male road cyclists (31.2 ± 9.1 years, 75.5 ± 7.5 kg, 178.4 ± 4.4 cm) conforming to Level 2 or greater (De Pauw et al., 2013) were recruited for this study. Level 2 is described as having a relative VO_{2max} between 45 and 54.9 ml/kg/min,

Table 1. General characteristics of cyclists (n = 17).

Variable	Mean ± SD
Age (years)	31.2 ± 9.1
Body mass (kg)	75.5 ± 7.5
Stature (cm)	178.4 ± 4.4
Percentage body fat (%)	8.4 ± 2.8
Trochanteric Leg Length (cm)	95.0 ± 2.7
Skinfolds (mm)	57.6 ± 15.4
PPO (W)	354.0 ± 34.5
PPO (W/kg)	4.7 ± 0.4
VO_{2max} (ml/kg/min) Relative	55.2 ± 6.4

and a relative Peak Power Output (PPO) between 3.6 and 4.5 W/kg. The general characteristics and performance parameters of the 17 cyclists are shown in Table 1. Prior to testing, each participant was informed of the risks and stresses associated with participation in the research trial, were personally interviewed about their training history, completed a Physical Activity Readiness Questionnaire (PAR-Q) (Whaley, Brubaker, & Otto, 2007) and signed an informed consent form. The study was approved by the Human Research Ethics Committee of the Faculty of Health Sciences of the University of Cape Town, and conformed to the principles of the World Medical Association Declaration of Helsinki (World Medical Association, 2013).

Testing procedure

The participants reported to the laboratory on three separate occasions (one week apart, over three weeks) with their own cycling shoes and pedals. A CycleOps 400 Indoor Pro Cycle (Power Tap: Saris Cycling Group®. Madison, WI. USA) was used for all trials. Saddle height, saddle setback, handlebar reach and handlebar height were set to match the configuration of the participant's own bicycle as previously described (Holliday et al., 2017).

On the first visit to the laboratory, the participant's anthropometric measurements were taken, followed by an incremental exercise test to volitional exhaustion. The Cycleops VirtualTraining app (VirtualTraining, version 1.7.3, Czech Republic) was used to control the ergometer and was set according to the participant's individual characteristics of age, mass and stature. Heart rate for all sessions was captured by a Suunto® T6C heart rate monitor (Suunto Oy, Vanata, Finland). The participant completed a PPO and Peak Oxygen Consumption test to determine the required workload for the experimental trials. The gas analysis was monitored over 15-s intervals using an on-line breath-by-breath gas analyser and pneumotach (Oxycon, Viasis, Hoechberg, Germany). Participants started exercising at a workload of 100 Watts and resistance was increased by continuous ramp protocol at a rate of 20 W every 60 s until the participant was exhausted and could not sustain a cadence of at least 60 revolutions per minute (rpm). PPO was calculated by averaging the power output for the final minute of the VO_{2peak} test. VO_{2peak} was recorded as the highest VO_2 reading recorded for 30 s during the test. The maximum heart rate (MHR) of each participant was calculated during the peak power output test, and was used to calculate the target heart rates for the intensity protocol.

On the second and third visit to the laboratory, the researcher attached the EMG and 3D motion capture markers to the participant (Hermens et al., 1999; "Plug-in Gait model details", 2008). This was followed by a static calibration of the motion capture system before the participant was seated on the CycleOps ergometer.

Each participant performed a 15-min exercise protocol at three different workload intensities based on the Lamberts Submaximal Cycle Test (Lamberts et al., 2009), which was previously demonstrated to be highly reliable, with an ICC of R = 0.96 and typical error of measurement less than 2 beats per minute (bpm). The first stage of the protocol involved cycling for 6 min at 60% MHR, followed immediately by 6 min at 80% MHR and a further 3 min at 90% MHR. Cyclists had to elicit and maintain their heart rate with resistance increased or decreased to avoid their heart rate deviating by more than 2 bmp. Participants were requested to maintain a cadence as close to 90 rpm as possible throughout the trial. Participants were instructed to remain seated and not to alter their riding position during the trial, i.e., no standing whilst pedalling or changing the handgrip position. The riding position was standardised with the cyclists hands on the brake hoods in order to avoid changes in metabolic cost due to modification of the trunk angle (Heil, Derrick, & Whittlesey, 1997).

Rating of Perceived Exertion (RPE) was recorded at the end of each intensity stage using the Borg 6–20 RPE scale (Borg, 1982). Power output, heart rate, speed, cadence and distance were recorded continuously for later analysis.

The participants repeated this procedure on a third visit to the laboratory one week later. By doing a repeat session, the reliability of the study's data was increased, suggesting that the hypothesised changes in kinematics may be reported with confidence and would also help to reduce the risk of errors in the data interpretation (Hopkins, 2013; Lamberts et al., 2009).

Instrumentation and analysis

Three-dimensional motion capture and EMG were recorded simultaneously during the second and third testing sessions. Data were recorded for 15 s during the second minute of each intensity interval, specifically at 2, 8 and 13 min. The 3D motion capture markers and EMG electrodes were placed by the primary investigator by measuring and recording the placement of each marker and electrode to increase the accuracy of placement in subsequent trials (Tsushima, Morris, & McGinley, 2003).

3D kinematics

An eight-camera motion capture system (Oxford Metric Vicon, Oxford, UK) was used to capture kinematic data and was recorded at a sampling rate of 250 Hz. The Vicon full body plug-in gait marker set allows for the measurement of all joint locations and angles of rotation as well as the calculation of joint moments. Plug-in Gait is a biomechanical model based on the Newington–Helen Hayes gait model that calculates joint kinematics and kinetics from the XYZ marker positions and specific subject anthropometric measurements. The standard full marker set was modified by placing the tenth thoracic (T10) vertebra marker over the fifth thoracic (T5) vertebra instead. This was done to more closely approximate static methods used to measure shoulder

flexion angle. All other joint angles and segments were defined as per the manual ("Plug-in Gait model details", 2008). Reflective markers were also placed on the pedal spindle and crank axis, to define a local coordinate system.

Analysis of the 3D kinematic data was performed using MATLAB (The Mathwork®, USA). The 3D kinematic data were low-pass filtered using a fourth-order Butterworth filter with a cut-off frequency of 12 Hz. Analysis of 10 revolutions from each intensity stage was performed on the range of the ankle, knee, hip, shoulder and elbow joint angles, as well as the lumbar and thoracic spine. Ankle and knee angles for each trial were reported at bottom dead centre (BDC) pedal position, determined as the point at which the pedal reflective marker reached its minimal vertical position, i.e., 180°. Full knee extension is equal to 0°. Ankle neutral is equal to 90° (dorsiflexion ≤90°, plantar-flexion >90°). The hip flexion angle for each trial was reported at top dead centre (TDC) pedal position, determined as the point at which the pedal reflective marker reached its maximal vertical position, i.e., 360°. Thoracic flexion was calculated relative to the local coordinate system, indicating a forward thoracic tilt or lean on the bicycle. Shoulder, elbow and spinal angles were taken as an average over the 360° cycle.

Electromyography

The EMG activity during the testing sessions was recorded using an 8-channel EMG system (Telemyo 2400 G2, Noraxon, USA, Inc., Arizona, USA) Two electrodes (Blue Sensor, Medicotest, Denmark) were placed on the belly of the right Gluteus Maximus (GMax), Vastus Medialis Oblique (VMO), Vastus Lateralis Oblique (VLO), Tibialis Anterior (TA), Rectus Femoris (RF), Medial Gastrocnemius (MG) and Biceps Femoris (BF) muscles. Prior to placing the electrodes on the skin, the skin over the muscle was shaved and cleaned with ethanol. The placement and location of the electrodes were according to the recommendations by SENIAM (Surface EMG for Non-invasive Assessment of Muscles) (Hermens et al., 1999).

All EMG activity was sampled at 1984 Hz, thus providing raw data at a high enough frequency for reliable data collection and quantitative data analyses. A 50 Hz notch filter was applied to filter out the power line noise. The signal was filtered using a 15–500 Hz band-pass filter to allow movement artefact below 15 Hz and non-physiological signals above 500 Hz to be removed. The data were smoothed using root mean squared analysis (RMS), which was calculated for a 50 ms window. Ten revolutions from each data set were used for EMG analysis, which was performed using MATLAB (The Mathwork®, USA). The processed EMG data were further analysed into each quadrant of the cycle revolution, where quadrant 1 represents 0–90°, quadrant 2: 90–180°, quadrant 3: 180–270° and quadrant 4: 270–360°. The average magnitude from each intensity level, from each quadrant, was expressed as a percentage of the average magnitude obtained during 10 full revolutions from the first intensity level.

For example, the average magnitude during the 80% intensity stage, in quadrant 3 was calculated as follows:

$$avg\ magnitude = \frac{\text{average of 10 revolutions during } \{80\%\} \text{ intensity stage in quadrant } \{3\}}{\text{average of10 revolutions during 60\% intensity stage over a full revolution}}\%$$

Statistical methods

All joint kinematic and EMG magnitude data are expressed as means ± standard deviation (mean ± SD). The data were statistically tested using a one-way ANOVA with repeated measures. When significant main effects were found, a Tukey test was used for post-hoc analysis. Significance was accepted when p value <0.05. The statistical analyses were performed using GraphPad Prism v7.0a (GraphPad Software, San Diego, CA, USA).

Results

The mean ± SD and p values for all the joint kinematics can be found in Table 2 and Figure 1. There was a significant change in all joints across all intensities, except for the hip and the shoulder joint. The ankle joint progressively moved into dorsiflexion with the increased intensity with a decrease in mean from 100 ± 5° at 60%, 97 ± 5° at 80% and 94 ± 6° at 90%, ($F(1.215, 27.95) = 26.79$). The knee flexion decreased progressively with an increase in intensity, with a decrease in mean from 37 ± 7° at 60%, 35 ± 6° at 80% and 34 ± 6° at 90%, ($F(1.75, 40.19) = 17.45$). The spinal flexion increased with an increase in intensity, with an increase from 45 ± 9° at 60%, 47 ± 11° at 80% and 48 ± 11° at 90%, ($F(1.68, 36.94) = 17.80$). The thoracic angle increased with an increase in intensity, with an increase in mean from 60 ± 5° at 60%, 62 ± 5° at 80% and 64 ± 5° at 90%, ($F(1.37, 30.16) = 21.59$). Elbow flexion increased progressively with increased intensity with an increase in mean from 31 ± 5° at 60%, 36 ± 5° at 80% and 43 ± 10° at 90%, ($F(1.23, 29.45) = 35.50$).

The mean ± SD and p values for all muscle EMG magnitudes can be found in Table 3 and Figure 2. There were significant changes in all muscle groups with increasing intensity. The change was most visible in the quadrant that the muscle has been shown to be most active in, and between 60% and 80% and 60% to 90% intensity. For example, VLO magnitude increased mostly in quadrant 1 which is the period during which knee extension is used to generate pedalling power.

Table 2. Mean ± standard deviation and p values for joint kinematics at different intensities and RPE.

	60%	80%	90%	p
Ankle BDC	100 ± 5	97 ± 5	94 ± 6	<0.0001$^{*\dagger\pm}$
Knee BDC	37 ± 7	35 ± 6	34 ± 6	<0.0001*†
Hip TDC	122 ± 6	122 ± 6	122 ± 6	0.856
Lumbar flexion	45 ± 9	47 ± 11	48 ± 11	<0.0001$^{*\dagger\pm}$
Thoracic lean	60 ± 5	62 ± 5	64 ± 5	<0.0001$^{*\dagger\pm}$
Shoulder	103 ± 9	104 ± 10	104 ± 8	0.815
Elbow	31 ± 5	36 ± 5	43 ± 10	<0.0001$^{*\dagger\pm}$
RPE	9 ± 1	13 ± 2	16 ± 2	<0.0001$^{*\dagger\pm}$
Average HR (bpm)	109 ± 6	144 ± 6	164 ± 7	<0.0001$^{*\dagger\pm}$
Average cadence (rpm)	88 ± 4	92 ± 2	92 ± 4	0.358
Average speed (km/hr)	36 ± 3	38 ± 4	35 ± 4	0.002$^{*\pm}$
Average power (W)	133 ± 17	240 ± 35	303 ± 45	<0.0001$^{*\dagger\pm}$

Significant change between 60 and 80% maximal heart rate (MHR), †significant change from 60% to 90% MHR, $^{\pm}$significant change between 80 and 90% MHR. RPE = Rate of perceived exertion. BDC = bottom dead centre. TDC = top dead centre.

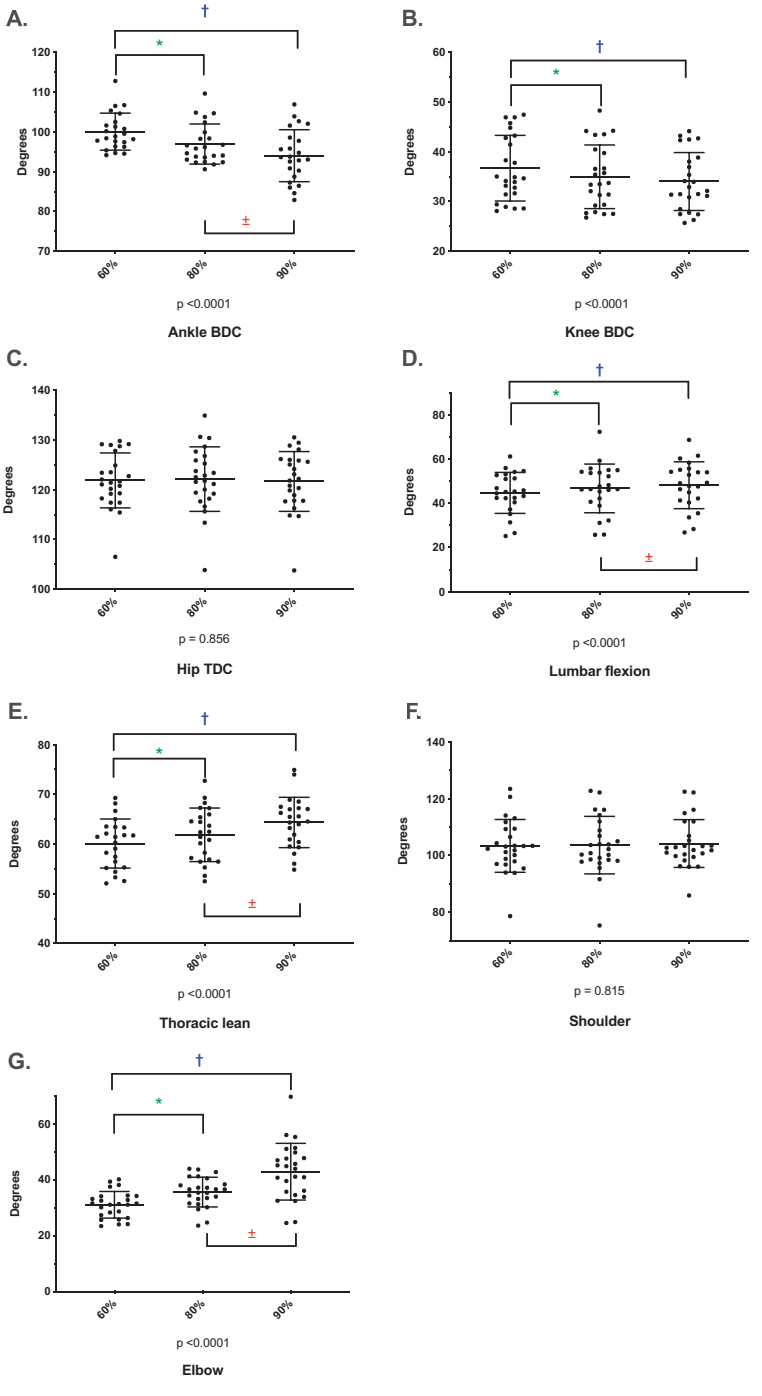

Figure 1. Joint angles over the different intensities with p values.

*Significant difference between 60% and 80% maximum heart rate (MHR), ±significant difference between 80% and 90% MHR, †significant difference between 60% and 90% MHR.

Table 3. Mean ± standard deviation in percentages for each muscle in each quadrant, and *p* value during each different intensity.

Muscle	Quadrant	60%	80%	90%	*p* value
GMax	0-90	232.60 ± 54.51	486.44 ± 165.64	624.37 ± 289.36	<0.0001$^{*\dagger\pm}$
	90-180	60.60 ± 24.34	138.42 ± 67.38	205.08 ± 93.85	<0.0001$^{*\dagger\pm}$
	180-270	40.31 ± 28.79	50.23 ± 36.69	59.17 ± 32.91	0.0007†
	270-360	57.63 ± 22.93	68.45 ± 35.53	82.22 ± 52.82	0.015$^{\dagger\pm}$
VMO	0-90	281.55 ± 26.97	387.97 ± 84.33	430.42 ± 114.39	<0.0001$^{*\dagger\pm}$
	90-180	37.16 ± 18.74	47.12 ± 23.55	54.00 ± 24.50	0.001*†
	180-270	9.92 ± 5.62	15.48 ± 9.52	18.99 ± 12.07	<0.0001$^{*\dagger\pm}$
	270-360	74.30 ± 25.20	104.06 ± 41.75	120.46 ± 69.23	0.006*†
VLO	0-90	280.88 ± 26.29	396.08 ± 90.17	471.79 ± 130.03	<0.0001$^{*\dagger\pm}$
	90-180	32.92 ± 16.27	43.86 ± 22.36	61.27 ± 47.42	0.009*†
	180-270	8.61 ± 3.06	11.86 ± 4.81	13.14 ± 5.02	<0.0001*†
	270-360	79.80 ± 21.61	112.33 ± 47.44	140.76 ± 71.31	0.0011*†
TA	0-90	61.85 ± 30.47	92.68 ± 59.60	106.75 ± 66.44	<0.0001$^{*\dagger\pm}$
	90-180	68.07 ± 39.44	87.41 ± 51.46	92.95 ± 54.12	0.051
	180-270	62.95 ± 32.32	78.30 ± 35.82	103.16 ± 63.33	0.029
	270-360	199.37 ± 52.00	267.89 ± 94.84	272.06 ± 132.52	0.017*
RF	0-90	146.17 ± 54.65	228.44 ± 142.76	296.10 ± 181.83	<0.0001$^{*\dagger\pm}$
	90-180	31.78 ± 16.95	37.76 ± 19.14	52.86 ± 26.60	<0.0001$^{*\dagger\pm}$
	180-270	64.42 ± 25.55	63.37 ± 29.74	68.19 ± 35.12	0.711
	270-360	156.95 ± 53.29	214.05 ± 89.06	244.66 ± 118.12	0.003*†
MG	0-90	77.12 ± 34.67	81.49 ± 34.07	85.20 ± 41.59	0.440
	90-180	259.81 ± 27.19	269.59 ± 43.28	259.77 ± 45.78	0.309
	180-270	52.93 ± 28.90	66.54 ± 33.32	75.24 ± 40.37	0.011†
	270-360	10.73 ± 4.44	12.71 ± 5.64	13.07 ± 5.45	0.025†
BF	0-90	121.07 ± 48.40	210.98 ± 73.27	293.15 ± 129.19	<0.0001$^{*\dagger\pm}$
	90-180	206.17 ± 57.91	325.20 ± 83.63	440.58 ± 145.11	<0.0001$^{*\dagger\pm}$
	180-270	45.14 ± 29.46	87.53 ± 62.95	129.06 ± 75.81	<0.0001$^{*\dagger\pm}$
	270-360	27.18 ± 7.40	43.93 ± 19.77	48.13 ± 23.06	<0.0001*†

Significant change between 60 and 80% MHR, †significant change from 60% to 90% MHR, $^{\pm}$ significant change between 80 and 90% MHR.

The rating of perceived exertion increased progressively and linearly in keeping with the increased intensity from a score of 9 ± 1 for 60%, 13 ± 2 for 80% and 16 ± 2 for 90% intensity (Table 2).

Discussion and implications

The ankle and knee normative values for static bike fitting have been well researched (Bini et al., 2011; Bini, Hume, Croft, & Kilding, 2011; Hamley & Thomas, 1967; Holmes, Pruitt, & Whalen, 1994; Peveler, 2008; Peveler et al., 2005, 2007) and more recently the difference between static and dynamic angles, specifically the ankle and knee, have been highlighted (Bini et al., 2016; Fonda et al., 2014; Holliday et al., 2017; Peveler et al., 2012). As yet there are no normative data to describe the dynamic values for full body joint angles recommended for cycling at differing intensities.

The muscle recruitment pattern during cycling has also been well researched (So et al., 2005), including intramuscular EMG (Chapman, Vicenzino, Blanch, Knox, & Hodges, 2010; Da Silva et al., 2016). The purpose of this study was not to report the activation patterns, but to assess the changes in the lower limb EMG magnitudes during differing intensities as it is not clear how these may change with the natural adoption of

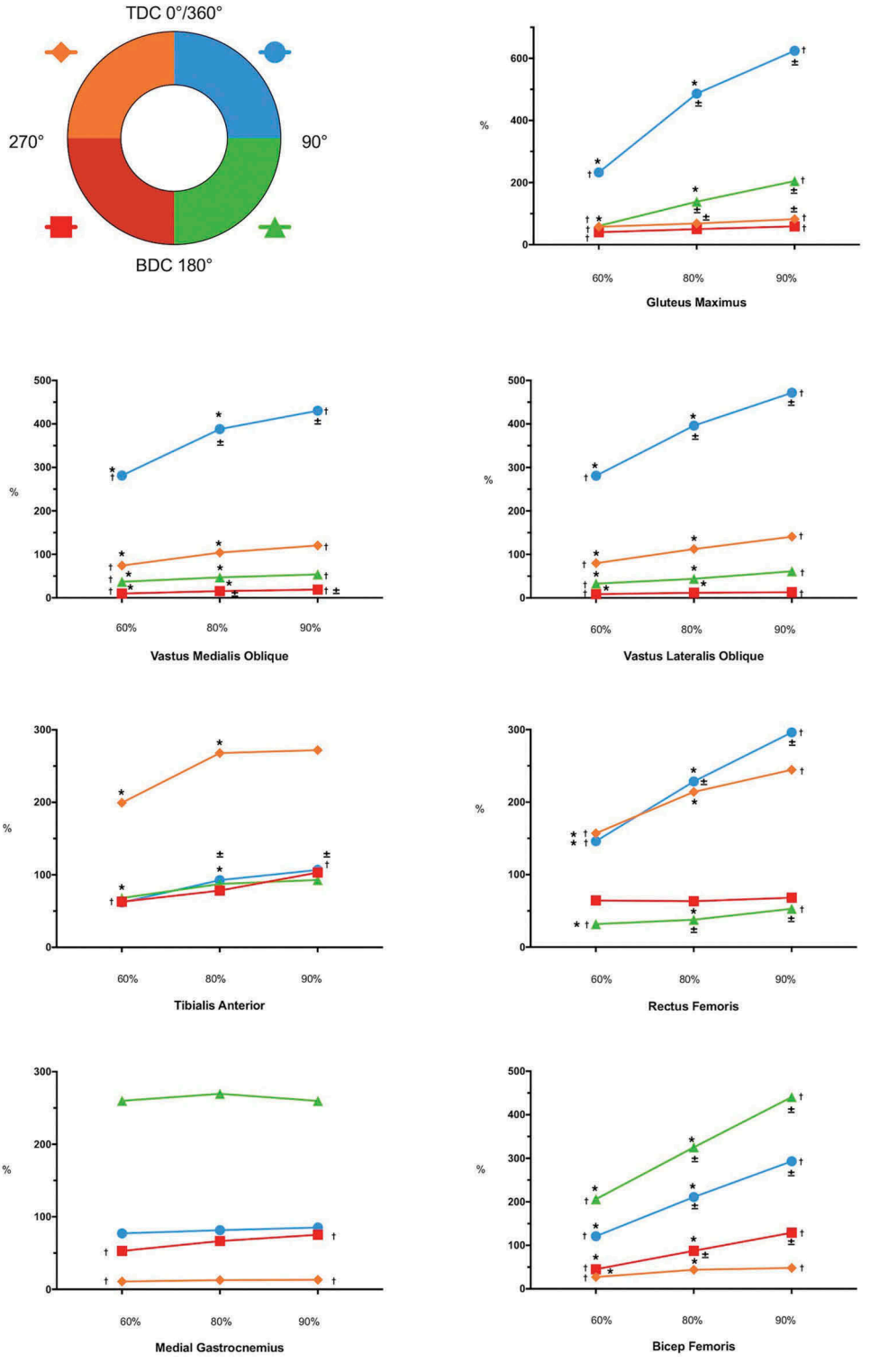

Figure 2. EMG magnitudes over different intensities, in each quadrant.

*Significant difference between 60% and 80% maximum heart rate (MHR), ±significant difference between 80% and 90% MHR, †significant difference between 60% and 90% MHR.

different body positions as intensities increase, nor whether the joint kinematics change significantly.

This study produced similar results to that of Blake et al. (2012), showing that there was a general increase in muscle activation across muscle groups as the intensity increased. Blake et al. (2012) analysed nine male cyclists at a low (25–55% VO_{2max}) and a high intensity (60–90% VO_{2max}). In keeping with this previous study, our study also demonstrated an increase in EMG activity of TA and RF across the top and early part of the pedal cycle (0–90°) with increasing intensity. TA was shown to work predominately in the fourth quadrant, thus suggesting an increase in ankle dorsiflexion near the TDC. There was a significant change in RF from 60% to 90% MHR in the first, second and fourth quadrants which correspond to hip flexion, driving the knee over the TDC of the pedal revolution and knee extension in the push phase. The significant changes in TA and RF may indicate that these are the muscles responsible for driving the pedal across the TDC, an area where the major muscle groups are unable to exert effective force to drive crank rotation.

The role of GMax is to extend the hip joint, and there were significant increases in EMG signal through all three intensities in the pushing phase of the pedal revolution (from 0° to 180°). Similarly, the VMO and VLO extend the knee joint in the same push phase of the pedal revolution, and there were significant increases in EMG magnitude through all three intensities in the first quadrant. The MG worked predominantly in the second quadrant, corresponding to the second half of the push phase of the pedal revolution; however, the magnitude remained constant with only minor significant changes in the third and fourth quadrants between 60% and 90%. Even though Soleus was not examined in this study, it has been demonstrated that Soleus and MG work together from 340° through to 270° in the pedal revolution to stabilise the ankle and to transfer force to the pedal exerted by the relatively large GMax and quadriceps muscles (Fonda & Sarabon, 2010; Jorge & Hull, 1986). As such, even at lower workloads the force applied by MG in order to stabilise the ankle may be relatively higher. Similar results have been reported by Blake et al. (2012) where GMax had the largest increase in activity from a low to a high intensity, VMO and VLO were both highly active in the push phase with increasing intensity and the MG showed very little change with increasing workloads.

Numerous studies have shown an increase in hip and knee extension, as well as ankle dorsiflexion, with incremental cycling (Bini et al., 2010; Bini & Diefenthaeler, 2010). The previous knee and ankle findings are consistent with our study, suggesting a movement into dorsiflexion to increase stability around the ankle joint in order to transfer force effectively to the pedals to maintain the power output. The movement into dorsiflexion may increase the efficiency of MG or increase passive tension in the muscle tendon unit to assist with force transfer. The ankle increased into dorsiflexion by 6° between 60% and 90% intensity, which is a greater difference than the reported TEM of 3.5° (Holliday et al., 2017). As the bicycle contact points are fixed, this increase in ankle dorsiflexion requires an increase in knee extension (Peveler et al., 2012). Dynamic bike fitting systems recommend a dynamic KFA of 30–40°, however there is no research validating this specific range. Previous research has demonstrated a difference in KFA of between 5° and 8° in static relative to dynamic measures (Farrell et al., 2003; Fonda et al., 2014; Holliday et al., 2017). The results from this

study also demonstrated a difference in KFA at low and high intensities, and it is, therefore, possible to infer that optimal KFA at BDC position using dynamic measurements should range from 33° to 43° at low intensity and 30–40° at high intensity. Although statistically significant, from a clinical and practical perspective, it is recommended that the use of dynamic 2D and 3D kinematic data should interpret knee flexion in relation to the relative intensity during data capture.

There were no significant hip joint angle changes in any of the quadrants, at any of the intensities. This differs from previous studies that have shown hip extension increases with incremental cycling (Bini et al., 2010; Bini & Diefenthaeler, 2010; Sanderson & Black, 2003). The hip angles in previous studies were measured as an angle bisecting the length of the femur and a line parallel to the floor or as an angle bisecting the length of the femur and a line from the hip joint centre to the shoulder centre. These measures exclude the spinal segments and do not measure the independent hip joint angle (long axis of femur and lumbar spine-sacrum), as was done in this study.

Similar to the hip, the shoulder angle is often determined as an angle between the elbow, mid-shoulder and hip joint centre. A clinical shoulder angle will take the thoracic spine into account, as was done in this study. There were no significant changes in the shoulder angle, at any of the different intensities, yet the elbow and thoracic lean angle changed significantly between all three intensities. This is consistent with research where there was a significant change in forward body position on the bicycle at maximal power output (Bini et al., 2012; Sayers & Tweddle, 2012). It was suggested that cyclists increased their trunk lean angle in response to muscular fatigue, and that changes in EMG preceded changes in mean trunk lean angle (Dingwell et al., 2008). It was hypothesised that the increase in trunk lean angle was in order to focus on increasing hip extensor muscle length and reducing knee flexor moment (Bini et al., 2012; Dingwell et al., 2008).

Our findings that the hip joint position remained unchanged while significant lumbar flexion did occur, indicate that the previous basic methods of measuring the angles of the body, without taking into consideration the spine, should be discarded. The spine consists of 33 bones and each joint has varying degrees of movement. It is clear from this study that movement occurs in the lumbar, thoracic and elbow joints with increased intensity, not at the hip or shoulder. A possible rationale for this change in position may relate to the transfer of force across the hip joint. GMax demonstrated the largest change in EMG magnitude from low to high workloads. Increased GMax activity may aid the transfer of the increased force across the hip joint by stabilising the pelvis (Li & Caldwell, 1998). The increase in lumbar flexion and elbow flexion may, therefore, be a compensatory mechanism to stabilise the pelvis through the contact points at the hands as the forces across the hip joint increase (Grant, Watson, & Baker, 2015). Future research on more detailed spinal segment kinematics as well as spinal and upper limb EMG analysis with increasing cycling intensity should be considered.

Conclusion

It is clear from this study that the magnitudes of muscles used during cycling increase with increasing intensity. The ankle adopts a more dorsiflexed position and the knee

moves into a more extended position with an increase in cycling intensity. The elbow and lumbar and thoracic spinal segments also adopt a more flexed position as intensity increases. Previous recommendations for optimal cycling position have been suggested for the lower limb, however from these results, it is essential that lumbar and thoracic spinal segments are also taken into account. Guidelines for optimal bicycle configuration should, therefore, consider the full body kinematics as well as conducting the bike fit at an intensity applicable to the cyclist's individual training and racing goals.

Disclosure statement

No potential conflict of interest was reported by the authors.

Funding

This work was supported by the National Research Fund of South Africa [101413].

References

Bini, R., Dagnese, F., Rocha, E., Silveira, M., Carpes, F., & Mota, C. (2016). Three-dimensional kinematics of competitive and recreational cyclists across different workloads during cycling. *European Journal of Sport Science*, *16*, 553–559. doi:10.1080/17461391.2015.1135984

Bini, R., & Diefenthaeler, F. (2010). Kinetics and kinematics analysis of incremental cycling to exhaustion. *Sports Biomechanics*, *9*, 223–235. doi:10.1080/14763141.2010.540672

Bini, R., Diefenthaeler, F., & Mota, C. B. (2010). Fatigue effects on the coordinative pattern during cycling: Kinetics and kinematics evaluation. *Journal of Electromyography and Kinesiology*, *20*, 102–107. doi:10.1016/j.jelekin.2008.10.003

Bini, R., Hume, P., & Croft, J. (2011). Effects of bicycle saddle height on knee injury risk and cycling performance. *Sports Medicine*, *41*, 463–476. doi:10.2165/11588740-000000000-00000

Bini, R., Hume, P., Croft, J., & Kilding, A. (2011). *Effects of saddle position on pedalling technique and methods to assess pedalling kinetics and kinematics of cyclists and triathletes* (PhD thesis). Auckland University of Technology.

Bini, R., Senger, D., Lanferdini, F., & Lopes, A. L. (2012). Joint kinematics assessment during cycling incremental test to exhaustion. *Isokinetics and Exercise Science*, *20*, 99–105. doi:10.3233/IES-2012-0447

Blake, O. M., Champoux, Y., & Wakeling, J. M. (2012). Muscle coordination patterns for efficient cycling. *Medicine and Science in Sports and Exercise*, *44*, 926–938. doi:10.1249/MSS.0b013e3182404d4b

Borg, G. (1982). Psychophysical bases of perceived exertion. *Medicine & Science in Sports & Exercise*, *14*, 377–381. doi:10.1249/00005768-198205000-00012

Burt, P. (2014). *Bike fit: Optimise your bike position for high performance and injury avoidance* (pp. 37–67). London: Bloomsbury Publishing Plc.

Chapman, A., Vicenzino, B., Blanch, P., Knox, J., & Hodges, P. (2010). Intramuscular fine-wire electromyography during cycling: Repeatability, normalisation and a comparison to surface electromyography. *Journal of Electromyography and Kinesiology*, *20*, 108–117. doi:10.1016/j.jelekin.2008.11.013

Da Silva, J., Tarassova, O., Ekblom, M. M., Andersson, E., Ronquist, G., & Arndt, A. (2016). Quadriceps and hamstring muscle activity during cycling as measured with intramuscular electromyography. *European Journal of Applied Physiology*, *116*, 1807–1817. doi:10.1007/s00421-016-3428-5

De Pauw, K., Roelands, B., Cheung, S., de Geus, B., Rietjens, G., & Meeusen, R. (2013). Guidelines to classify subject groups in sport-science research. *International Journal of Sports Physiology and Performance*, *8*, 111–122. doi:10.1123/ijspp.8.2.111

de Vey Mestdagh, K. (1998). Personal perspective: In search of an optimum cycling posture. *Applied Ergonomics*, *29*, 325–334. doi:10.1016/S0003-6870(97)00080-X

Dingwell, J., Joubert, J., Diefenthaeler, F., & Trinity, J. (2008). Changes in muscle activity and kinematics of highly trained cyclists during fatigue. *IEEE Transactions on Bio-Medical Engineering*, *55*, 2666–2674. doi:10.1109/TBME.2008.2001130

Dorel, S., Guilhem, G., Couturier, A., & Hug, F. (2012). Adjustment of muscle coordination during an all-out sprint cycling task. *Medicine and Science in Sports and Exercise*, *44*, 2154–2164. doi:10.1249/MSS.0b013e3182625423

Farrell, K. C., Reisinger, K. D., & Tillman, M. D. (2003). Force and repetition in cycling: Possible implications for iliotibial band friction syndrome. *Knee*, *10*, 103–109. doi:10.1016/S0968-0160(02)00090-X

Ferrer-Roca, V., Roig, A., Galilea, P., & Garcia-Lopez, J. (2012). Influence of saddle height on lower limb kinematics in well-trained cyclists: Static versus dynamic evaluation in bike fitting. *Journal of Strength and Conditioning Research*, *26*, 3025–3029. doi:10.1519/JSC.0b013e318245c09d

Fonda, B., & Sarabon, N. (2010). Biomechanics of cycling. *Sports Science Review*, *XIX*, 187–210. doi:10.2478/v10237-011-0012-0

Fonda, B., Sarabon, N., & Li, F. (2014). Validity and reliability of different kinematics methods used for bike fitting. *Journal of Sports Sciences*, *32*, 940–946. doi:10.1080/02640414.2013.868919

Grant, M., Watson, H., & Baker, J. (2015). Assessment of the upper body contribution to multiple-sprint cycling in men and women. *Clinical Physiology and Functional Imaging*, *35*, 258–266. doi:10.1111/cpf.12159

Hamley, E., & Thomas, V. (1967). Physiological and postural factors in the calibration of the bicycle ergometer. *Journal of Physiology*, *191*, 55–56.

Heil, D., Derrick, T., & Whittlesey, S. (1997). The relationship between preferred and optimal positioning during submaximal cycle ergometry. *European Journal of Applied Physiology and Occuptional Physiology*, *75*, 160–165. doi:10.1007/s004210050141

Hermens, H. J., Freriks, B., Merletti, R., Stegeman, D., Blok, J., Rau, G., … Hägg, G. (1999). *European recommendations for surface electroMyoGraphy*. Enschede, the Netherlands: Roessingh Research and Develpoment.

Holliday, W., Fisher, J., Theo, R., & Swart, J. (2017). Static versus dynamic kinematics in cyclists: A comparison of goniometer, inclinometer and 3D motion capture. *European Journal of Sport Science*, *17*, 1129–1142. doi:10.1080/17461391.2017.1351580

Holmes, J., Pruitt, A., & Whalen, N. (1994). Lower extremity overuse in bicycling. *Clinics in Sports Medicine*, *13*, 187–205.

Hopkins, W. (2013). A new view of statistics. Retrieved from http://www.sportsci.org/resource/stats/relycalc.html

Hug, F., & Dorel, S. (2009). Electromyographic analysis of pedaling: A review. *Journal of Electromyography and Kinesiology*, *19*, 182–198. doi:10.1016/j.jelekin.2007.10.010

Jorge, M., & Hull, M. (1986). Analysis of EMG measurements during bicycle pedalling. *Journal of Biomechanics*, *19*, 683–694. doi:10.1016/0021-9290(86)90192-2

Kay, D., Marino, F. E., Cannon, J., St Clair Gibson, A., Lambert, M. I., & Noakes, T. D. (2001). Evidence for neuromuscular fatigue during high-intensity cycling in warm, humid conditions. *European Journal of Applied Physiology*, *84*, 115–121. doi:10.1007/s004210000340

Lamberts, R. P., Swart, J., Richard, W., Hons, M., Noakes, T. D., & Lambert, M. I. (2009). Measurement error associated with performance testing in well- trained cyclists : Application to the precision of monitoring changes. *International SportMed Journal*, *10*, 33–44.

Li, L., & Caldwell, G. (1998). Muscle coordination in cycling: Effect of surface incline and posture. *Journal of Applied Physiology*, *85*, 927–934. doi:10.1152/jappl.1998.85.3.927

Padilla, S., Mujika, I., Orbananos, J., Santisteban, J., Angulo, F., & Goiriena, J. (2001). Exercise intensity and load during mass-start stage races in professional road cycling. *Medicine & Science in Sports & Exercise*, *33*, 796–802. doi:10.1097/00005768-200105000-00019

Palmer, G., Hawley, J., Dennis, S., & Noakes, T. (1994). Heart rate responses during a 4-d cycle stage race. *Medicine and Science in Sports and Exercise*, *26*, 1278–1283. doi:10.1249/00005768-199410000-00016

Peveler, W. (2008). Effects of saddle height on economy in cycling. *Journal of Strength and Conditioning Research*, *22*, 1355–1359. doi:10.1519/JSC.0b013e318173dac6

Peveler, W., Bishop, P., Smith, J., Richardson, M., & Whitehorn, E. (2005). Comparing methods for setting saddle height in trained cyclists. *Journal of Exercise Physiology Online*, *8*, 51–55.

Peveler, W., Pounders, J., & Bishop, P. (2007). Effects of Saddle Height on anaerobic power production in cycling. *Journal of Strength and Conditioning Research*, *21*, 1023–1027. doi:10.1519/R-20316.1

Peveler, W., Shew, B., Johnson, S., & Palmer, T. (2012). A kinematic comparison of alterations to knee and ankle angles from resting measures to active pedaling during a graded exercise protocol. *Journal of Strength and Conditioning Research*, *26*, 3004–3009. doi:10.1519/JSC.0b013e318243fdcb

Plug-in Gait model details. (2008, March). Retrieved from Vicon website www.vicon.com/downloads/documentation/plug-in-gait-model-details

Sanderson, D. J., & Black, A. (2003). The effect of prolonged cycling on pedal forces. *Journal of Sports Sciences*, *21*, 191–199. doi:10.1080/0264041031000071010

Sayers, M., & Tweddle, A. (2012). Thorax and pelvis kinematics change during sustained cycling. *International Journal of Sports Medicine*, *33*, 314–390. doi:10.1055/s-0031-1291363

Silberman, M., Webner, D., Collina, S., & Shiple, B. (2005). Road bicycle fit. *Clinical Journal of Sport Medicine*, *15*, 271–276.

So, R., Ng, J., & Ng, G. (2005). Muscle recruitment pattern in cycling: A review. *Physical Therapy in Sport*, *6*, 89–96. doi:10.1016/j.ptsp.2005.02.004

Tsushima, H., Morris, M. E., & McGinley, J. (2003). Test-retest reliability and inter-tester reliability of kinematic data from a three-dimensional gait analysis system. *Journal of the Japanese Physical Therapy Association*, *6*, 9–17. doi:10.1298/jjpta.6.9

Whaley, M., Brubaker, P., & Otto, R. (2007). Preparticipation health screening and risk stratification. In M. Whaley, P. Brubaker, & R. Otto (Eds.), *ACSM's guidelines for exercise testing and prescription* (pp. 26). Philadelphia: Lippincott Williams & Wilkins.

World Medical Association. (2013). World medical association declaration of Helsinki: Ethical principles for medical research involving human subjects. *Journal of the American Medical Association*, *310*, 2191–2194. doi:10.1001/jama.2013.281053